

nated with a retrograde pathway that recycles vesicle proteins and retrieves escaped ER residents (19). Indeed, selective exclusion of secretory cargo from retrograde vesicles may explain the concentration of certain soluble cargo after export from the ER (5). Our results indicating Erv29p action as a cargo receptor do not exclude other sorting mechanisms; rather, it now seems probable that multiple mechanisms of retention, retrieval, and selective export operate in concert to achieve organization of the early secretory pathway.

References and Notes

1. G. Warren, I. Mellman, *Cell* **98**, 125 (1999).
 2. M. J. Kuehn, J. M. Herrmann, R. Schekman, *Nature* **391**, 187 (1998).
 3. S. Springer, R. Schekman, *Science* **281**, 698 (1998).
 4. W. E. Balch, J. M. McCaffery, H. Plutner, M. G. Farquhar, *Cell* **76**, 841 (1994).
 5. J. A. Martinez-Menarguez, H. J. Geuze, J. W. Slot, J. Klumperman, *Cell* **98**, 81 (1999).

6. M. Muniz, C. Nuoffer, H.-P. Hauri, H. Riezman, *J. Cell Biol.* **148**, 925 (2000).
 7. C. Barlowe *et al.*, *Cell* **77**, 895 (1994).
 8. S. Otte *et al.*, *J. Cell Biol.* **152**, 503 (2001).
 9. J. E. Reeves, M. Fried, *Mol. Membr. Biol.* **12**, 201 (1995).
 10. S. R. Caldwell, K. J. Hill, A. A. Cooper, *J. Biol. Chem.* **276**, 23296 (2001).
 11. C. Barlowe, *J. Cell Biol.* **139**, 1097 (1997).
 12. D. Julius, R. Schekman, J. Thorner, *Cell* **36**, 309 (1984).
 13. T. Stevens, B. Esmon, R. Schekman, *Cell* **30**, 439 (1982).
 14. W. J. Belden, C. Barlowe, unpublished data.
 15. S. Y. Bednarek *et al.*, *Cell* **83**, 1183 (1995).
 16. C. Appenzeller, H. Andersson, F. Kappeler, H. P. Hauri, *Nature Cell Biol.* **1**, 330 (1999).
 17. W. C. Nichols *et al.*, *Cell* **93**, 61 (1998).
 18. K. J. Travers *et al.*, *Cell* **101**, 249 (2000).
 19. H. R. Pelham, *Curr. Opin. Cell Biol.* **7**, 530 (1995).
 20. For data plots of the experiments in Figs. 2 and 3, see *Science* Online (www.sciencemag.org/cgi/content/full/294/5546/1528/DC1).
 21. Strain CBY966 (10) was transformed with pAC530 (12) to generate CBY1160 (*erv29Δ::KAN ERV29-HA*). FY834 (10) was transformed with pDA6300 (*Mfx1-*

LEU2-2μ) to generate CBY1161. CBY1162 contains *pRS306-ERV29* integrated into the *URA3* locus of CBY1161.

22. Antiserum to Erv29p was raised against a GST-Erv29p fusion protein. A 262-base pair 5' Apo I fragment from *ERV29* was inserted into pGEX-5x-3, and fusion protein was purified as described by the manufacturer (Amersham Pharmacia). Antiserum was produced in rabbits by Covance Inc. (Denver, PA).
 23. Cross-linking reactions (0.05 ml) were performed in buffer 88 [25 mM Hepes (pH 7.5), 150 mM KOAc, 0.25 M sorbitol, and 5 mM MgOAc] for 20 min at 20°C. Reactions were quenched with 10 mM glycine for 5 min at 20°C, solubilized with an equal volume of 1% SDS, and heat-denatured. Where indicated, proteins were immunoprecipitated with antibodies after dilution with 1 ml of IP buffer [15 mM Tris-Cl (pH 7.5), 150 mM NaCl, and 1% Triton X-100].
 24. We thank A. Cooper for providing the HA-tagged Erv29p construct, R. Gilmore for antiserum to CPY, and R. Schekman for antiserum to αf. Supported by grants from the National Institute of General Medical Sciences and the Pew Scholars Program in the Biomedical Sciences.

9 August 2001; accepted 28 September 2001

Lack of Acrosome Formation in Hrb-Deficient Mice

Ningling Kang-Decker,¹ George T. Mantchev,¹ Subhash C. Juneja,¹ Mark A. McNiven,^{2,3} Jan M. A. van Deursen^{1*}

The sperm acrosome is essential for sperm-egg fusion and is often defective in men with nonobstructive infertility. Here we report that male mice with a null mutation in *Hrb* are infertile and display round-headed spermatozoa that lack an acrosome. In wild-type spermatids, *Hrb* is associated with the cytosolic surface of proacrosomic transport vesicles that fuse to create a single large acrosomic vesicle at step 3 of spermiogenesis. Although proacrosomic vesicles form in spermatids that lack *Hrb*, the vesicles are unable to fuse, blocking acrosome development at step 2. We conclude that *Hrb* is required for docking and/or fusion of proacrosomic vesicles during acrosome biogenesis.

The acrosome is a unique membranous organelle that is formed during spermiogenesis through an integrated process of transport vesicle production, trafficking, and fusion (1, 2). In the first period of acrosome biogenesis, the Golgi phase, numerous small proacrosomic vesicles accumulate in the medulla, a cytoplasmic compartment located between the juxta-nuclear Golgi apparatus and the nuclear surface. There, they coalesce into a single spherical acrosomic vesicle that attaches to the nucleus. During the subsequent Cap phase, the acrosomic vesicle expands by means of sustained vesicular membrane transport and fusion. At the onset of sperm elongation, the acrosomic vesicle stops growing in size and starts undergoing a series of

highly complex morphological changes that shape the sperm cell. Little is known about the molecular mechanisms that regulate the targeting and fusion of transport vesicles during acrosomic vesicle formation, although the understanding of this process is highly relevant because disturbances of acrosomal development and function perturb the fertilizing capacity of spermatozoa (3, 4).

Here we identify the Asn-Pro-Phe (NPF) motif-containing protein *Hrb* (also called Rab or hRip) (5–7) as a component that is essential for acrosome formation. We addressed the physiological role of *Hrb* through targeted inactivation of the *Hrb* gene in the mouse (8, 9). *Hrb*^{-/-} mice were indistinguishable from *Hrb*^{+/-} and *Hrb*^{+/+} mice, had a normal life-span, and showed no apparent histological abnormalities in brain, colon, heart, kidney, liver, lung, spleen, or thymus. Western blot analysis confirmed that the mutant *Hrb* allele was null (8, 9). Despite normal sexual behavior and copulation, *Hrb*^{-/-} males derived from two independently targeted embryonic stem cell (ES) clones were infertile.

By contrast, *Hrb*^{-/-} females displayed normal fertility. The average testicular weight in 10-week-old *Hrb*^{-/-} mice [0.079 g ± 0.1 (n = 12 testes)] was not significantly different from that in wild-type mice [0.082 g ± 0.09 (n = 12 testes)]. However, *Hrb*^{-/-} mice contained on average ~15-fold less spermatozoa in the cauda epididymis than wild-type males (8). The spermatozoa from mutant males showed severely reduced motility and several structural abnormalities. The spermatozoa displayed a globic head (Fig. 1A) with a round nucleus and a tail midpiece lacking the mitochondrial sheath (Fig. 1B) (8). This sheath is composed of mitochondria that generate adenosine triphosphate (ATP) for movement of the flagellum and is formed in the final steps of normal spermatid elongation (2). In vitro fertilization experiments revealed that *Hrb*^{-/-} spermatozoa were unable to establish sperm-egg attachment and fertilization (Fig. 1C) (8).

β-galactosidase staining of the testis of *Hrb*^{+/-} mice indicated that the *Hrb* gene was abundantly transcribed during spermiogenesis (9). Histological analysis of testis sections showed that seminiferous-tubule diameters in *Hrb*^{+/+} and *Hrb*^{-/-} mice were comparable (9). The number and distribution of mitotic (spermatogonia) and meiotic (spermatocytes) germ cells in these tubules also appeared to be similar (Fig. 2, A and B) (8). The appearance of interstitial cells was also normal. However, the process of transformation of round spermatids into testicular spermatozoa (spermiogenesis) was clearly disrupted in *Hrb*^{-/-} mutants. Typically, mutant tubules were devoid of elongated spermatids and contained exclusively round-headed spermatids (Fig. 2B) (9). Although acrosomes were easily detectable in wild-type round spermatids by light microscopy and by transmission electron microscopy (TEM) (Fig. 2, A and C) (8), no acrosome structures were visible in mu-

¹Department of Pediatrics and Adolescent Medicine, ²Department of Biochemistry and Molecular Biology, ³Department of Gastroenterology and Hepatology, Mayo Clinic, 200 First Street SW, Rochester, MN 55905, USA.

*To whom correspondence should be addressed. E-mail: vandeursen.jan@mayo.edu

REPORTS

tant spermatids (Fig. 2, B and D). Extensive ultrastructural analysis of testis sections by TEM showed normal spermatogenesis in knockout mice up through the second step of spermiogenesis, when numerous small proacrosomic vesicles accumulate in the medulla. However, these vesicles failed to fuse with each other to yield the single large acrosomic vesicle found in normal spermiogenesis (Fig. 2, E through J). This stage-specific defect was consistent in both lines of *Hrb*^{-/-} mice (*n* = 5 mice). These results suggest that the primary spermatogenic defect in *Hrb*^{-/-} mice is an arrest in acrosomic vesicle biogenesis at step 2 of spermiogenesis caused by defective docking and/or fusion of proacrosomic vesicles.

To further characterize the role of *Hrb* in acrosome formation, we determined the intracellular localization of the protein in wild-type spermatids by immunofluorescence confocal microscopy (8). *Hrb*-specific immunoreactivity appeared in several small punctae throughout the cytoplasmic compartment of round spermatids. A high concentration of punctae consistently appeared in the medulla, as revealed by double labeling of round spermatids for *Hrb* and Golgi-membrane 58-kD protein (Fig. 3A). As

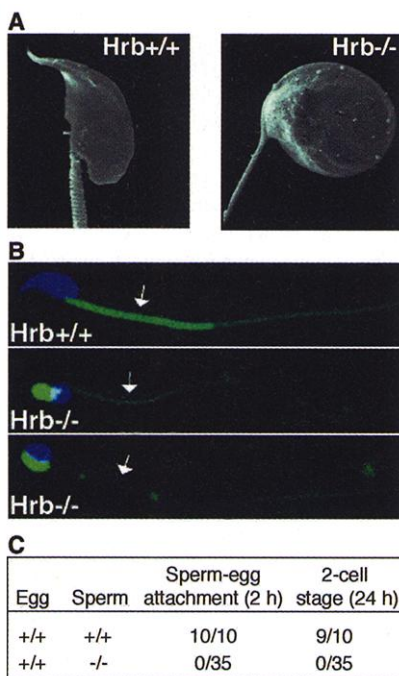


Fig. 1. Analysis of spermatozoa from *Hrb*-deficient mice. (A) Scanning electron micrographs of sperm cells in the cauda epididymis of wild-type and knockout mice. (B) Mitochondrial sheath configurations in *Hrb*^{+/+} and *Hrb*^{-/-} spermatozoa. Mitochondria (arrows) were stained with MitoTracker Green (green). Nuclei were stained with Hoechst (blue) to visualize the sperm heads. (C) In vitro fertilization experiments with zona pellucida-intact eggs from wild-type females and sperm from *Hrb*^{+/+} or *Hrb*^{-/-} males. Sperm-egg interaction and fertilization were determined by microscopy at 2 and 24 hour post-insemination, respectively.

Fig. 2. *Hrb*^{-/-} round spermatids lack an acrosome. (A and B) Cross sections through seminiferous tubules from 10-week-old *Hrb*^{+/+} (A) and *Hrb*^{-/-} (B) males stained with toluidine blue. Indicated are positions of interstitial cells (I), spermatogonia (Sg), spermatocytes (Sc), round-headed spermatids (RS), and elongated spermatids (ES). Arrowheads point to acrosomes of round spermatids. (C through J) Transmission electron micrographs of round spermatids from 10- or 12-week-old *Hrb*^{+/+} and *Hrb*^{-/-} mice. (C) Section through a step 6 *Hrb*^{+/+} spermatid with a flat, cap-like acrosome (*). Note the thin layer of electron dense material on the inner aspect of the nuclear envelope below the acrosome. This layer is typically present throughout steps 3 through 12 of spermiogenesis, but not at steps 1 and 2. (D) Arrested *Hrb*^{-/-} round spermatid without an acrosome. (E) Medulla of a *Hrb*^{+/+} spermatid at step 2 with many proacrosomic vesicles. (F) Medulla of a step 2 *Hrb*^{-/-} spermatid showing a high concentration of proacrosomic vesicles. (G) Step 4 *Hrb*^{+/+} spermatid with a newly formed acrosome (hemispherical). (H) *Hrb*^{-/-} spermatid with small proacrosomic vesicles that target to the NE, but fail to fuse. (I) Step 6 *Hrb*^{+/+} spermatid containing a cap-like acrosome. (J) *Hrb*^{-/-} spermatid with proacrosomic vesicles along the NE. Abbreviations are as follows: G, Golgi apparatus; Nu, nucleus; NE, nuclear envelope; AC, acrosome; M, medulla; P, large proacrosomic vesicle with an electron dense core. Arrowheads point out the NE.

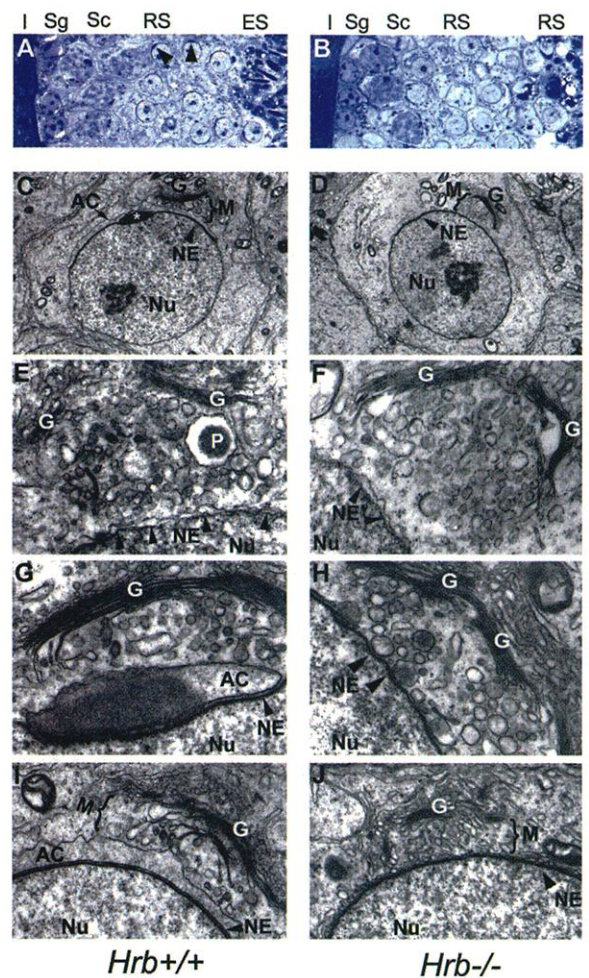
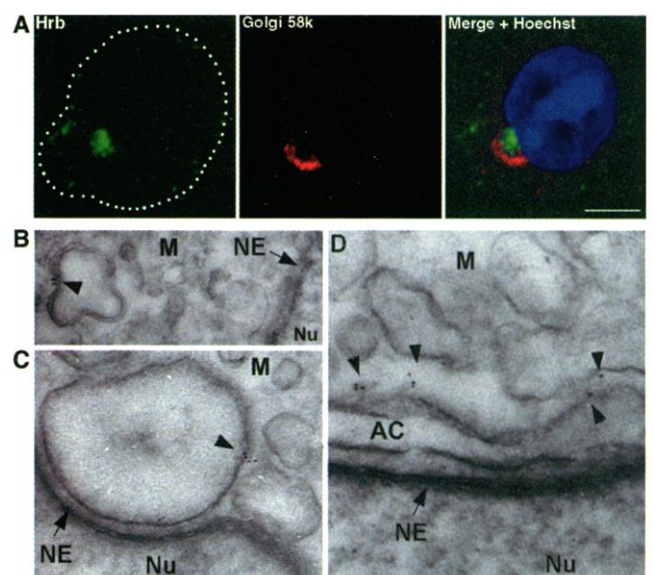
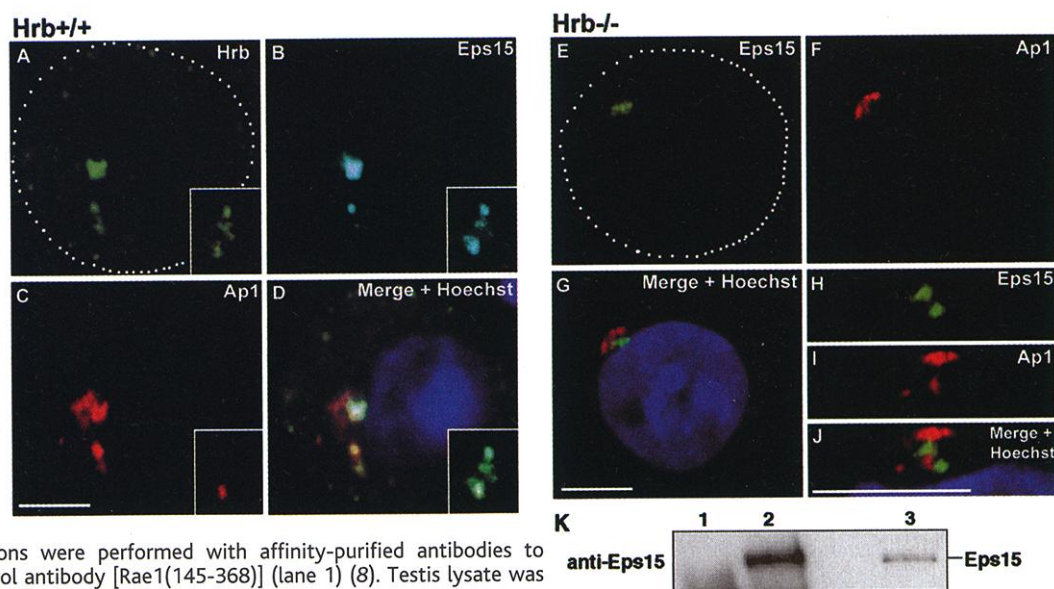


Fig. 3. *Hrb* is associated with membranous organelles in the medulla of round spermatids. (A) Confocal images of a wild-type round spermatid after immunofluorescent staining with *Hrb* and Golgi 58 K protein. Bar, 5 μm. (B through D) Immunoelectron micrographs of *Hrb*^{+/+} round spermatids. We visualized *Hrb* by incubating a testicular germ cell suspension first with affinity-purified *Hrb* antibody and then with antibody to rabbit immunoglobulin G (IgG) covalently linked to 5-nm gold particles. (B) Detail of a step 2 spermatid, showing *Hrb* at the surface of a relatively large proacrosomic vesicle. (C) A step 3 spermatid with newly formed acrosomic vesicle settling at nuclear envelope. (D) A round spermatid with a cap-like acrosome exhibiting *Hrb* labeling at the cytoplasmic surface of the acrosomic vesicle. Arrowheads highlight the gold particles. Abbreviations are as indicated in Fig. 2.



REPORTS

Fig. 4. The medulla of $Hrb^{-/-}$ spermatids lacks Ap1/Eps15 double-positive vesicles. (A through D) Confocal images of a representative $Hrb^{+/+}$ round spermatid triple-labeled with Hrb (A), Eps15 (B), and Ap1 (C) antibodies. Note that the medulla section shown in the large images contains punctae that are $Hrb^{+}/Eps15^{+}/Ap1^{+}$ or $Ap1^{+}$. The insets show a distinct medulla section with several $Hrb^{+}/Eps15^{+}$ punctae. (D) Merged images. (E through J) Confocal images of representative $Hrb^{-/-}$ round spermatids double-labeled with Eps15 (E) and (H) and Ap1 (F) and (I) antibodies. (G) and (J) Merge images. Bar, 5 μ m. (K) Interaction between Eps15 and Hrb in mouse testis. Immunoprecipitations were performed with affinity-purified antibodies to Hrb(386-562) (lane 2) or to control antibody [Rae1(145-368)] (lane 1) (8). Testis lysate was loaded to mark the position of Eps15 on the blot (lane 3).



expected, no Hrb labeling was detected in $Hrb^{-/-}$ round spermatids (data not shown). We further defined these Hrb-positive punctae by immunoelectron microscopy (IEM) (8). Labeling for Hrb was associated with the cytosolic surface of proacrosomic vesicles of early round spermatids (Fig. 3, B and C). In round spermatids with a developing acrosomic vesicle, gold particles were also found at distinct positions along the outer membrane of the acrosomic vesicle (Fig. 3D). These findings suggest that Hrb may function in vesicle-to-vesicle docking and/or fusion during acrosome biogenesis.

Next, we investigated the relation between Hrb and Eps15, a transport vesicle adaptor protein with a role in endocytosis and vesicle sorting that has been shown to interact with Hrb and several other NPF proteins by virtue of its Eps15 homology (EH) domains (7, 10). We demonstrated that Hrb and Eps15 form a complex in testis by a coimmunoprecipitation approach (8) (Fig. 4K). We then used immunofluorescence confocal microscopy to determine whether Eps15 and Hrb colocalize during the process of acrosome biogenesis. Eps15 appeared prominently in small punctae in the medulla that generally coincided with Hrb. Measurements revealed that of 177 punctae in 30 round spermatids, 150 (85%) labeled for both Hrb and Eps15. Only 20 and 7 punctae were only positive for Hrb or Eps15, respectively. Triple labeling (8) of round spermatids for Hrb, Eps15, and Ap1, a heterotetrameric adaptor protein complex that is associated with Golgi-derived transport vesicles, showed that more than half (62%) of the $Hrb^{+}/Eps15^{+}$ punctae in the medulla also contained Ap1 (Fig. 4, A through D). Furthermore, we observed that a relatively small number of punctae [43 of 220 punctae (20%); $n = 30$ round spermatids] contained only Ap1. Unlike Ap1, Ap2, a marker for endocytic vesicles, did not exhibit any punctate

labeling in round spermatids. These results suggest that the medulla of round spermatids contains distinct subsets of proacrosomic vesicles that are $Hrb^{+}/Eps15^{+}/Ap1^{+}$, $Hrb^{+}/Eps15^{+}$, or $Ap1^{+}$. When we labeled Hrb-deficient round spermatids for Ap1 and Eps15, both adaptor proteins exhibited a punctate staining in the medulla, but there was no appreciable overlap between the Eps15 and Ap1 staining patterns (Fig. 4, E through J). Specifically, of 345 punctae in 37 spermatids, only 7 (2%) contained both Eps15 and Ap1, whereas 159 (46%) were positive only for Eps15 and 179 (52%) only for Ap1. This strictly separate distribution of Eps15 and Ap1 suggests that Eps15-positive proacrosomic vesicles lack the ability to merge with Ap1-positive proacrosomic vesicles in the absence of Hrb and further supports the idea that Hrb is a critical component of the vesicle-to-vesicle docking and/or fusion machinery that forms the acrosomic vesicle.

Our studies demonstrate the critical role of Hrb in acrosomic vesicle formation during early mouse spermiogenesis. The primary defect in proacrosomic vesicle fusion seems to affect male fertility at the levels of sperm-egg fusion, sperm movement, and sperm number. The sperm acrosome is known to be critical for sperm-egg fusion (1), and the complete lack of this organelle in $Hrb^{-/-}$ spermatozoa explains why no sperm-egg fusion occurred in our in vitro fertilization experiments. The poor motility of $Hrb^{-/-}$ spermatozoa is apparently due to lack of the mitochondrial sheath in the tail midpiece. Formation of this tail structure is dependent on sperm elongation, which, in turn, depends on acrosomic vesicle formation (2). Hence, poor motility of $Hrb^{-/-}$ spermatozoa is probably a secondary consequence of the step 2 arrest in acrosome biogenesis. A decrease in sperm count appears to be a common phenotype for a variety of genetic defects perturbing the normal differ-

entiation program of mouse spermiogenesis (11). Therefore, the reduced sperm count of $Hrb^{-/-}$ males is probably also a secondary effect of the acrosomal defect. Because healthy heterozygous and homozygous female and heterozygous male mice can easily transmit Hrb null alleles to the progeny, similar mutations in humans may also be highly transmissible. They may, in fact, account for some of the idiopathic human infertility syndromes associated with reduced sperm count and production of round-headed spermatozoa (3). The developmentally abnormal round spermatids from $Hrb^{-/-}$ males may be valuable for further testing and improvement of human infertility treatments that are based on round spermatid injection (12).

References and Notes

1. A. Abou-Haila, D. R. Tulsiani, *Arch. Biochem. Biophys.* **379**, 173 (2000).
2. Y. Clermont, L. Oko, L. Hermo, *Cell Biology of Mammalian Spermiogenesis* (Oxford Univ. Press, New York, ed. 2, 1993), p. 332-376.
3. W. B. Schill, *Hum. Reprod.* **6**, 969 (1991).
4. G. Singh, *Int. J. Fertil.* **37**, 99 (1992).
5. H. P. Bogerd, R. A. Fridell, S. Madore, B. R. Cullen, *Cell* **82**, 485 (1995).
6. C. C. Fritz, M. L. Zapp, M. R. Green, *Nature* **376**, 530 (1995).
7. A. E. Salcini *et al.*, *Genes Dev.* **11**, 2239 (1997).
8. For the methods used, see supplementary information at *Science Online* (9).
9. Supplementary material is available on *Science Online* at www.sciencemag.org/cgi/content/full/294/5546/1531/DC1.
10. T. de Beer *et al.*, *Nature Struct. Biol.* **7**, 1018 (2000).
11. J. P. Venables, H. J. Cooke, *J. Endocrinol. Invest.* **23**, 584 (2000).
12. J. Tesarik, C. Mendoza, J. Testart, *N. Engl. J. Med.* **333**, 525 (1995).
13. B. Hogan, R. Bedington, F. Constantini, E. Lacy, *Manipulating the Mouse Embryo* (Cold Spring Harbor Laboratory Press, Cold Spring Harbor, NY, ed. 2, 1994).
14. We thank B. Cullen for the human Hrb/Rab cDNA. We thank R. Bram, F. Couch, H. Cao, L. Iverson, E. Krueger, T. Trejo, and J. van Ree for critically reviewing our manuscript or helpful discussions, and R. Mantcheva for animal care.

21 June 2001; accepted 5 October 2001